Organisms Diversity & Evolution (2024) 24:1–15
https://doi.org/10.1007/s13127-023-00635-6

ORIGINAL ARTICLE

Bumps on the back: An unusual morphology in phylogenetically distinct *Peridinium* aff. *cinctum* (= *Peridinium tuberosum*; Peridiniales, Dinophyceae)

Selin Gürkan[1] · Benedikt Stemplinger[1] · Alexander Rockinger[1] · Johanna Knechtel[1] · Marc Gottschling[1]

Received: 16 March 2023 / Accepted: 14 December 2023 / Published online: 20 January 2024

Abstract

To determine the intraspecific variability of microscopic organisms such as dinophytes is challenging, but can be achieved using cultured material. Unusual morphologies of *Peridinium tuberosum* assigned to the *Peridinium cinctum* species group have been described as bulges on the posterior end of the cell a hundred years ago and more, but its taxonomic significance is unclear at present. We collected field material in Germany and Poland in order to establish strains to study cell morphology using light and scanning electron microscopy. For the cultured material, DNA sequence data from the rRNA operon was gained as well and included in molecular phylogenetics (including 22 new partial rRNA sequences). Two new, closely related ribotypes were detected, and all strains showed the principle morphology of *P. cinctum* having an asymmetric epitheca, a large first apical plate and a sulcus extending onto the epitheca. In the single-strain GeoM*979 assigned to one of the two new ribotypes, cells with bulges appeared rarely but consistently, mostly on the hypotheca, but other variations also occurred. Overall, cells of this strain display traits not observed before while studying cultured *P. cinctum*, and this distinction is further supported by molecular data and additional details of epithecal opening. However, there does not remain enough information to determine strain GeoM*979 as a separate species (namely *P. tuberosum*) and therefore, it is identified as *Peridinium* aff. *cinctum* until further notice.

Keywords Dinoflagellate · Molecular sequence diagnostics · Morphology · Phylogeny · Provisional name · Taxonomy

Introduction

Despite its ecological importance, species delimitation and identification of microscopic organisms such as dinophytes are no easy task to achieve (Manoylov, 2014; Morrison et al., 2009; Wilson, 2017). This is particularly true for many historical taxa, which have been described during the nineteenth and twentieth centuries (Kretschmann, Žerdoner Čalasan et al., 2018; Tillmann et al., 2019). At that time, contemporary methods were still not established, and taxonomic delimitation heavily depended on the morphospecies concept based on structural traits only. Cells were observed in an environmental sample that contained numerous different organisms, making it difficult to recognise intraspecific variability. Later, the cultivation of monoclonal strains allowed for consideration of intraspecific variability during morphological observations (Burkholder & Glibert, 2006; Kretschmann et al., 2022), which is combined with DNA sequence analysis today (Hebert et al., 2003).

The success of molecular data has brought discussions to employ the ribosomal ITS region as a species-specific marker in dinophytes (Gottschling et al., 2005; Ott et al., 2022; Stern et al., 2012). Molecular data analysis has helped tremendously to distinguish species (Kretschmann, Owsianny et al., 2018; Tillmann et al., 2014), but it also highlights some challenges, as the morphological analysis does not always correspond to molecular data. Molecular analysis has brought awareness to cryptic species that are genetically discernible but indistinguishable in morphology (Gottschling et al., 2005; Litaker et al., 2009; Montresor et al., 2003). An opposite case is seen in *Apocalathium* Craveiro, Daugbjerg, Moestrup & Calado: Despite their almost identical rRNA sequences, species differ in their morphology and ecology (Annenkova et al., 2015). Occasionally, dinophyte populations show also intraspecific variability of the rRNA operon, and different ribotypes are found in the same species (Izquierdo López et al., 2018;

✉ Marc Gottschling
gottschling@bio.lmu.de

[1] Department Biologie, Systematics, Biodiversity & Evolution of Plants, GeoBio-Center, Ludwig-Maximilians-Universität München, Menzinger Str. 67, D-80 638 Munich, Germany

Kremp et al., 2014; Nguyen-Ngoc et al., 2021). All these examples show that the application of molecular data as a unique identifier of species depends on the particular case. The best way of species identification is to follow the biological species concept (Mayr, 1942): Individuals belonging to distinct species cannot reproduce or produce sterile offspring, but this criterion is methodologically challenging to apply in dinophytes or unicellular organisms in general.

Peridinium cinctum (O.F.Müll.) Ehrenb. (Peridiniaceae) is a common dinophyte with a considerably wide distribution in freshwater habitats of both temperate and tropical areas (Ehrenberg, 1832; Izquierdo López et al., 2018; Moestrup & Calado, 2018). The species inhabit eu- through oligotrophic water bodies with pH values varying from 4 to 8 (Moestrup & Calado, 2018). Its remarkable ability to adapt to the surrounding conditions with almost no limits is described by Höll (1928). The dinophyte cell is circular in outline and divided by a cingulum into two parts. The cellulosic plates on the upper part are defined as epitheca and the plates on the lower part as hypotheca, whereas the epitheca has an asymmetrical plate pattern. The Kofoidean plate formula of the epitheca is 4′, 3a, 7″, first determined by Stein (1883), and the first apical plate is relatively large in comparison to the supposed close relative of *P. cinctum*, *Peridinium gatunense* Nygaard. The sulcus of *P. cinctum* extends onto the epitheca, which is larger than the hypotheca. Due to areolation, the surface of the cells appears wrinkled.

The intraspecific variability within *P. cinctum* has been a topic of interest for more than 100 years and investigated also in recent years. Morphologically, plate splits and fusions in epithecal conformations are documented as well as shifts of specific sutures between the plates, and a considerable number of subspecific taxa at the rank of, for example, variety and form has been introduced in the past (Lefèvre, 1932; Lindemann, 1917, 1920). Izquierdo López et al. (2018) and Romeikat et al. (2019), who observed thousands of cells, combined such morphological approaches with rRNA sequence data exhibiting five ribotypes. However, there are no correlations between morphology, genetic disposition or distribution resulting in a species concept of *P. cinctum*, for which a high intraspecific variability in various regards is assumed (Izquierdo López et al., 2018).

Some varieties of *P. cinctum* with an unusual morphology are also known. Cells with an epithecal plate pattern of *P. cinctum* but with 'three massive protuberances emerging from the antapical cone as a tripod' (Meunier, 1919: 53; Fig. 1) have been described as *Peridinium tuberosum* Meunier from Belgium. The protologue could be interpreted as provisional, in original words 'nous l'appelons provisoirement Per. tuberosum' (Meunier, 1919, p. 53), with the result that the name is not validly published based on Art. 36.1 (a) (see also Ex. 5) of the *International Code of Nomenclature for algae, fungi, and plants* (ICN; Turland et al., 2018). However, Article 36.1 was amended in Shenzhen to make it clearer that the criterion was whether or not the author was accepting the name rather than the specific words being used (although the existing examples were not reviewed to see if they reflected the new wording, *pers. comm.* John McNeill and Nicholas Turland)—thus, there should be no doubt but that *P. tuberosum* (and its combinations to a variety: Lindemann, 1928, and a form: Lefèvre, 1932, under *P. cinctum*) is validly published. The name(s) were used by subsequent authors (Moestrup & Calado, 2018; Schiller, 1937; Киселев, 1950), also in some studies (Graffius, 1966; Carty, 2008; Shams et al., 2012, occasionally not presenting the distinctive morphology described above: Baykal & Açıkgöz, 2004; Baykal et al., 2004). Meunier (1919, p. 12) did not provide precise measurements either for *P. tuberosum* or for other organisms he described (transl. 'We therefore refrain from stating the sizes in micromillimetres, this only leaves inaccurate ideas in the mind').

In this study, we present the morphology of the strain GeoM*979, some of whose cells have bulge-like structures erupting from the posterior end. We provide DNA sequence information associated with this unusual morphology, which appears consistent with the descriptions of *P. tuberosum* (Meunier, 1919). We further present the morphology of strains, which are closely related to GeoM*979 based on molecular sequence data, but do not show hypothecal protuberances. Our results expand the knowledge of dinophyte diversity, but species delimitation between *P. cinctum* and its putative relatives remains challenging.

Materials and methods

Strain GeoM*979 was established by micropipetting from field material collected at Lake Wojnowickie (Poland, Greater Poland, Leszno) on Jun 6, 2018. Seven additional strains were established from field material collected at the Jägerweiher (Germany, Rhineland-Palatinate, Ludwigshafen) on Jan 21, 2022. Cultivation using freshwater WC growth medium (Woods Hole Combo, modified after Guillard & Lorenzen, 1972) without silicate took place in climate chambers at 18 °C and 12 °C, respectively, and a 12:12 h light:dark photoperiod. The strains (Table S1) are currently held in the culture collection at the Institute of Systematics, Biodiversity and Evolution of Plants (University of Munich) and are available upon request. Strain GeoM*979 is additionally available as CCAC9309B at the Central Collection of Algal Cultures (University of Duisburg-Essen), as CCAP1140/12 at the Culture Collection of Algae and Protozoa (Dunbeg) and as CCCM6036 at the Canadian Center for the Culture of Microorganisms (Vancouver).

Cells were observed and documented with a CKX41 inverse microscope (Olympus; Hamburg, Germany) equipped

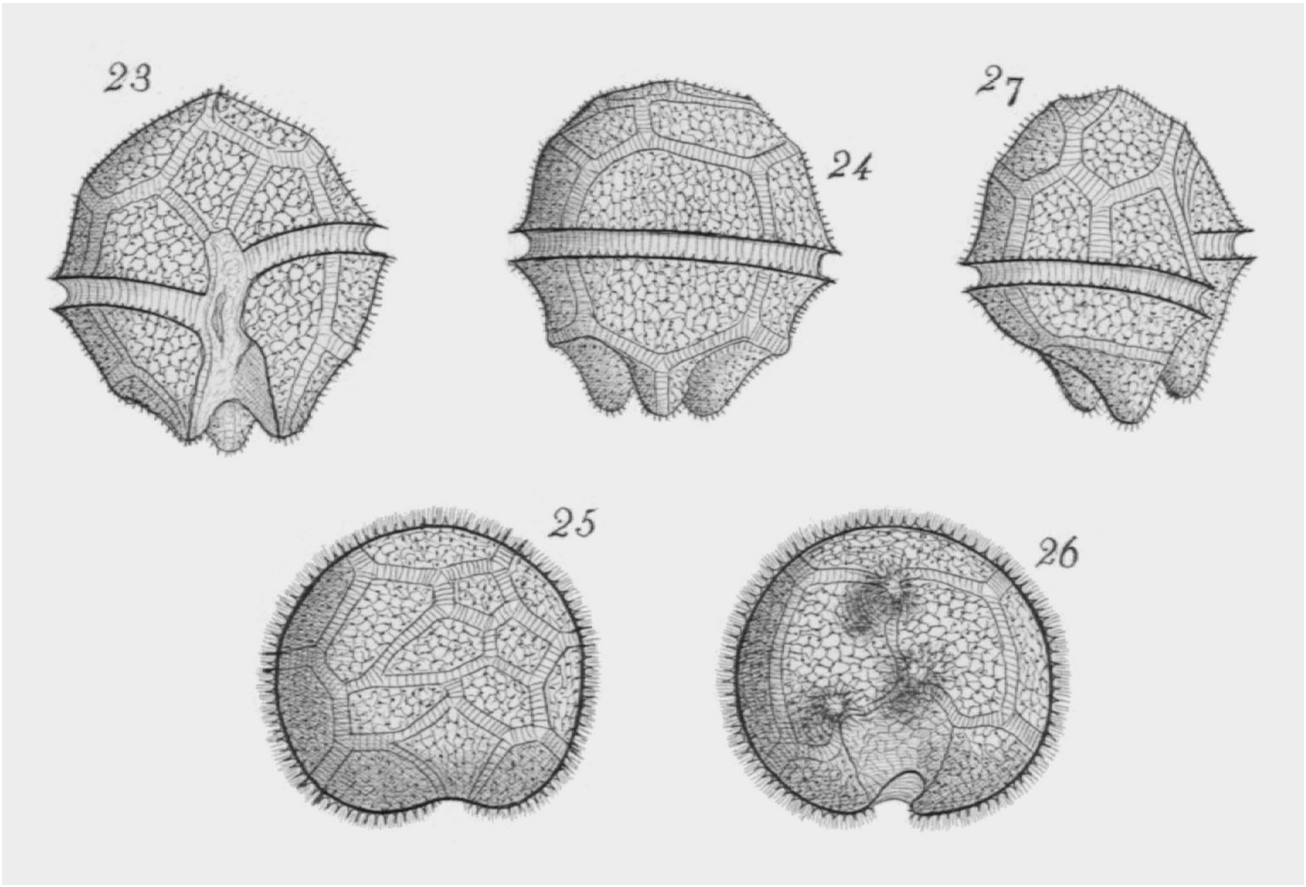

Fig. 1 The original material of *Peridinium tuberosum*. Numbers indicated by Meunier (1919) follow: (23) Ventral view with sulcus extending onto the epitheca (similar to *Peridinium cinctum* but different from *Peridinium gatunense*). (24) Dorsal view. (25) Apical view with asymmetrical epithecal plate pattern (similar to *P. cinctum*). (26) Antapical view. (27) Right lateral view with a slight tilt towards the front. Note the bulges on the posterior end of the cell in 23−24, 26−27, which are distinctive traits of *P. tuberosum*

with a phase-contrast option. Images were taken with a DP73 digital camera (Olympus) and if applicable, samples were covered with a droplet of Protogel (Protist Motility Inhibitor C340, Sciento; Manchester, UK). For nuclear staining, cells were treated with 4′-6-diamidino-2-phenylindole (DAPI, 10 µg ml^{-1} final concentration) for 10 min. For visualisation of the nuclei, and also for observing chloroplasts of motile cells applying autofluorescence, a DM1000 light microscope (Leica; Wetzler, Germany) equipped with a DAPI filter (Leica; excitation: 350/50, dichroic mirror: 400, emission BP 460/50) and an I3 filter (Leica; excitation: 450/490, dichroic mirror: 510, emission LP 515) was used as described previously (Romeikat et al., 2020). Measurements were made using the programs 'cellSens Entry' (Olympus) and 'Fiji' (https://imagej.net/software/fiji/).

For the preparation of permanent slides, cells of the strain GeoM*979 were fixed with 2.5% glutaraldehyde (Plano; Wetzlar, Germany). Double-staining was performed using 0.5% (water-based) astra blue in 2% tartaric acid (Fluka; Buchs, Switzerland) in WC medium and 0.1% (ethanol-based) eosin (Merck; Darmstadt, Germany) during a graded ethanol (Roth; Karlsruhe, Germany) series. Ethanol-based Technovit 7100 (Heraeus; Wehrheim, Germany) was used for embedding, following the manufacturer's instructions. For the final specimens, 40 µl aliquots of the Technovit mixture including the embedded samples were transferred to three microscopic slides. The specimens are deposited at the Centre of Excellence for Dinophyte Taxonomy (CEDiT; Wilhelmshaven, Germany), and duplicates are held in Berlin, B and Munich, M.

Preparation for scanning electron microscopy (SEM) followed standard protocols (Gottschling et al., 2012; Janofske, 1992). Cells were centrifuged at 500 rpm for 10 min and afterwards, it was fixed in 2.5% glutaraldehyde overnight. The next day, the cells were filtered onto an OmniporeTM membrane filter (5 µm, Merck) placed in a Swinnex® 130 filter holder (Merck) and washed three times in cacodylate buffer in 5 min and 2 × 15 min intervals. The same washing steps were repeated in distilled water in 5 min and 15 min intervals. Cells were dehydrated

using a graded acetone series (Roth) in 15 min intervals (10%, 30%, 50%, 70%, 90%). Then, 100% acetone was used for the last dehydration step, repeated three times in 5 min and 2 × 30 min intervals. After critical point drying (K850 Critical Point Dryer, Quorum; Lewes, UK), cells were sputter-coated (BAL-TEC SCD 050; Schalksmühle, Germany) with platinum on an aluminium stub and mounted using Planocarbon (Plano). The material was observed with the SEM LEO438VP (LEO Electron Microscopy; Cambridge, England, UK). All images were adjusted in Photoshop (Adobe Systems; Munich, Germany) and arranged with QuarkXPress (Quark Software; Hamburg, Germany).

DNA harvest and isolation, as well as PCR amplification and sequencing, are described previously (Izquierdo López et al., 2018). To build the alignment, we defined three regions of the rRNA: SSU, ITS, LSU and included a systematically representative set of Peridiniaceae (Table S1, including information on the outgroup comprising Heterocapsaceae and Protoperidiniaceae), similar as previously compiled and covering the known rRNA diversity of Peridiniaceae (Holzer et al., 2022) and all ribotypes of *P. cinctum* (Izquierdo López et al., 2018) from various European regions (no rRNA sequence information is available from outside Europe). Phylogenetic analyses were the same as those applied in Holzer et al. (2022). Secondary structures of ITS sequences (Gottschling & Plötner, 2004) were predicted using the Mfold software (Zuker, 2003; http://www.unafold.org/mfold/applications/rna-folding-form.php).

Results

Strain GeoM*979

The strain GeoM*979 displayed flagellated, thecate cells (Figs. 2, 3b–c, f and 4) and coccoid cells (Fig. 3g, e), with thecate cells being predominant. Within the culture vessels, the flagellated cells swam often towards the light source. Living cells during exponential growth had numerous golden through olive-brown chloroplasts (Figs. 2a, c, e, 3a, c–d, g and 4a–c). The nucleus was semi-anular (rectangular with rounded angles in the outline of dorsal or ventral view) and had a median, horizontal position (Fig. 2d). Accumulation bodies with an orange or reddish colour were spotted in several cells (Figs. 2a, e, 3c–d, g and 4a). Cells in the stationary growth phase contained a high number of necrotic cells (Fig. 4d), and chloroplasts of such cells appeared grey.

An apical pore was absent in all thecate cells (Figs. 2g, 3b and 4h), and the surface of the cellulosic plates was areolate. The sulcus extended onto the epitheca as a narrow slit (Fig. 2e–f, j). The epithecal plate pattern was asymmetrical and presented the Kofoidean formula 4′, 3a, 7″ (Figs. 2g, 3b and 4h). Taking the suture extending from plate 1′ as a median plane, the kite shape of plate 3′ and the elongated plates 4′ and 3a disturbed the symmetry of the epitheca. The pattern of the hypotheca was also asymmetrical with plate 2‴′ being larger than plate 1‴′ (Figs. 2k and 4g).

Fig. 2 Flagellated cells of strain GeoM*979. **a**–**f** Light microscopy, **g**–**m** scanning electron microscopy, **a**–**d** images taken from the same cell. **a** Dorsal view. **b**–**c** Chloroplasts (as inferred from autofluorescence) at two different focal planes, note the space occupied by the nucleus. **d** Cell nucleus with chromosomes (as inferred from astra blue staining). **e** Ventral view of living cell. **f** Empty theca (mirrored) portraying cellular plates on the ventral side. **g** Apical view. **h** Dorsal view. **j** Ventral view. **k** Antapical view. **l** Right lateral view. **m** Left lateral view. Plate labelling follows the Kofoidean notation, n′: apical plate; n″: precingular plate; n‴; postcingular plate; n⁗: antapical plate; na: anterior intercalary plate; sp: posterior sulcal plate. Scale bar = 10 µm

Two distinct cell morphologies of the thecate cells could be distinguished. Approximately 95% of the cells showed a regular appearance, and the remaining cells had bulges of various shapes and positions on the cell body. The regular cells were circular in outline and dorsoventrally flattened (Fig. 2l–m). Within these cells, no distinct size classes were observed: Cell length ranged between 40 and 53 µm (mean, 46 µm; median, 46 µm; SD, 4.0 µm; $n = 50$) and width between 37 and 48 µm (mean, 43 µm; median, 42 µm; SD, 3.5 µm; $n = 50$). Having no difference in motility, tabulation pattern or chloroplast traits compared to the regular form, cells with bulges were rare but unmistakably appeared in every culture vessel. The frequency of such cells usually was 5%, with the highest abundance of 10% in the exponentially growing, cultured cells of May 2021 (this material was taken for SEM examination). Maintenance time of a newly inoculated strain did not seem to affect the appearance of cells with bulges and also in stationary growth phase, necrotic cells with bulges could be observed (Fig. 4d). Cell length ranged from 40 to 58 µm including the bulges (mean, 47 µm; median, 47 µm; SD, 5 µm; $n = 50$) and from 36 to 52 µm in width (mean, 41 µm; median, 40 µm; SD, 4 µm; $n = 50$) being only marginally different from the regular cells.

The appearance of bulges was variable ($n = 50$): They were considerably large and present either on the hypotheca only (50%; Fig. 4a–b, e–g) or on both hemispheres (40%; Fig. 4c–d, j) or on the epitheca only (10%). Observations in SEM showed that a single bulge arose from a particular thecal plate (Fig. 4e–j). The number of bulges per cell was not constant, varied between one and three and was rarely four (Fig. 4). If present on the hypotheca ($n = 45$), then two bulges on plate 1‴′ and 2‴′ (60%), one bulge on either plate 1‴′ or 2‴′ (31%, rarely on plate 5‴′: Fig. 4g) or three bulges (9%) were counted. If present on the epitheca ($n = 25$), then three (44%), two (24%), one (24%; Fig. 4h–j) or more bulges (8%) were counted on different plates.

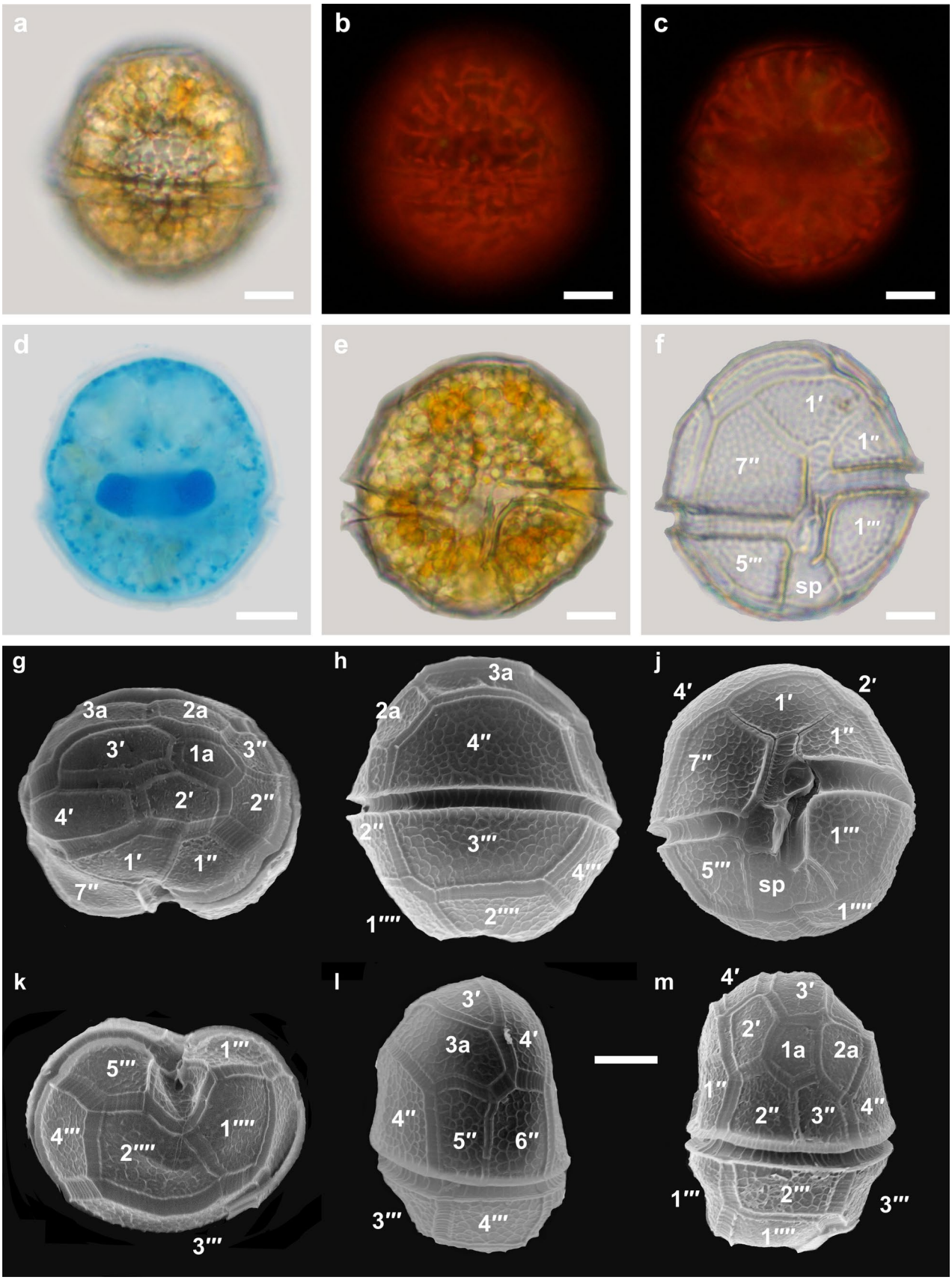
a
b
c
d
e
f
1′
1″
7″
1‴
5‴
sp
g
3a
2a
3′
1a
3″
4′
2′
2″
1′
1″
7″
h
3a
2a
4″
2″
3‴
4‴
1⁗
2⁗
j
4′
1′
2′
1″
7″
1‴
5‴
sp
1⁗
k
1‴
5‴
4‴
1⁗
2⁗
3‴
l
3′
3a
4′
4″
5″
6″
3‴
4‴
m
4′
3′
2′
1a
2a
1″
2″
3″
4″
1‴
2‴
3‴
1⁗

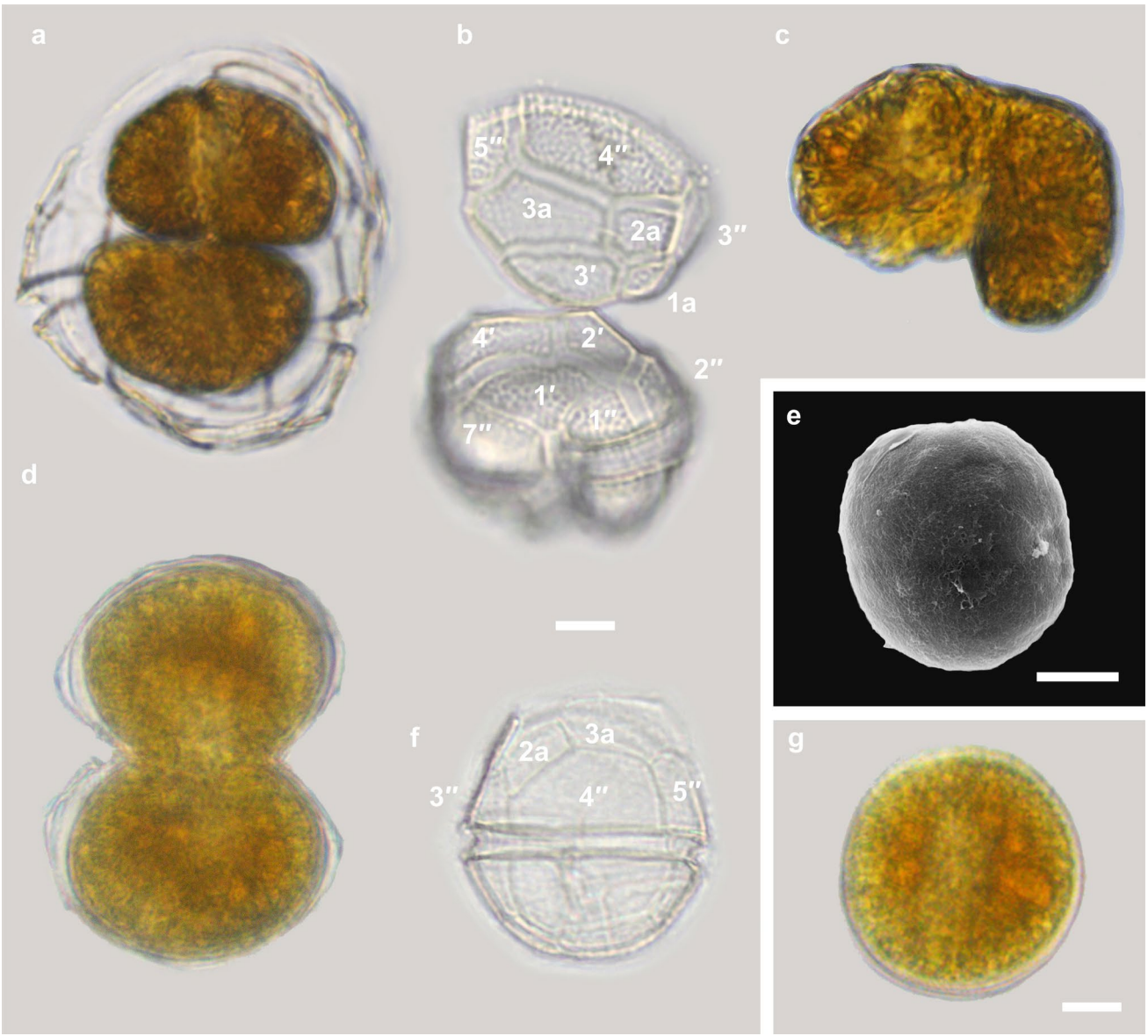

Fig. 3 Developmental stages of strain GeoM*979. **a**–**d**, **f**–**g** Light microscopy, **e** scanning electron microscopy. **a** Two thecate cells enclosed in the parental theca. **b** Opened theca, ventral view, note that opening starts from the dorsal part of the cell and the lid composed of the plates 3′, 1a–3a, 3″–5″. **c** Two connected, swimming cells. **d** Two connected, immotile cells enclosed in the parental thecae. **e** Coccoid cell. **f** Opened theca, dorsal view, note that a ventral lid is removed and the dorsal part still connected to the hypotheca. **g** Coccoid cell. Plate labelling follows the Kofoidean notation, n′: apical plate; n″: precingular plate; na: anterior intercalary plate. Scale bar = 10 µm

Cell division was by eleuteroschisis. Empty thecae discarded by the cells formed clumps and could then be spotted with the naked eye. Nearly all thecae opened from the dorsal part of the epitheca, and epithecal plates disintegrated frequently into separated pieces. Only in some cases, larger parts remained intact, such as a lid of plates comprising plates 3′, all intercalary plates and plates 3″–5″ and as the other piece the hypotheca, the cingular plates and plates 1′–2′, 4′, 1″–2″ and 6″–7″ (Fig. 3b, f). Several cells enclosed in their parental theca were spotted either as pairs (Fig. 3a) or individually (Fig. 3d). Occasionally, two connectedly swimming cells were observed (Fig. 3c): These cells were bigger than an average cell across the strain and had two longitudinal flagella. In the presence of a light source, a portion of such cells swam away from the light, while some slowed down and eventually accumulated under the light source. The fate of the presumable zygotes was not determined.

Coccoid cells were globose or ovoid and had a smooth surface (Fig. 4e, g). Their length ranged from 31 to 57 µm

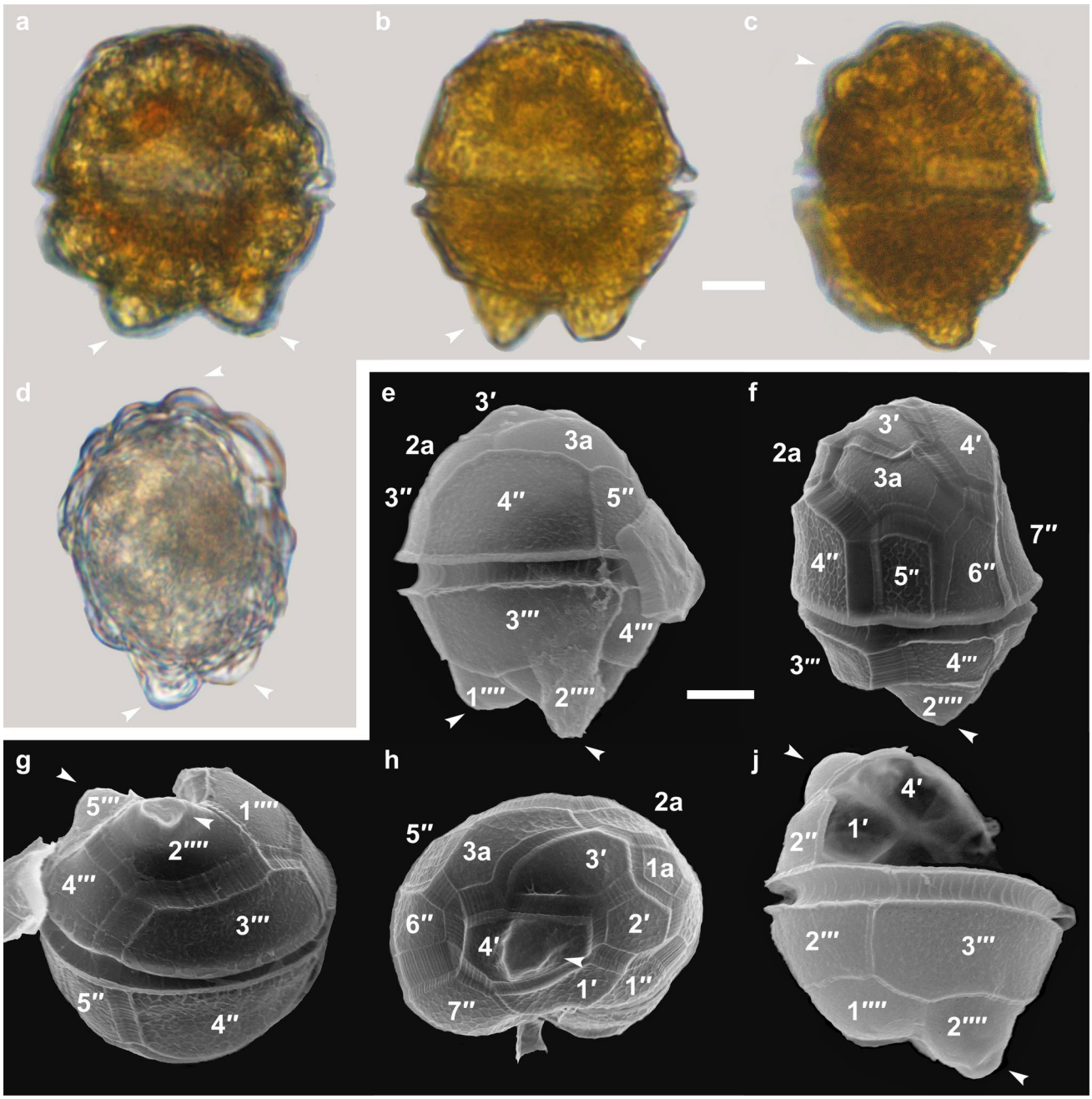

Fig. 4 Cells with bulges of strain GeoM*979. **a**–**d** Light microscopy, **e**–**j** scanning electron microscopy; bulges are indicated by arrows. **a**–**b** Different shapes and colours of cells with two bulges on hypotheca. **c** Vital cell with bulges on epi- and hypotheca. **d** Necrotic cell with bulges on epi- and hypotheca. **e** Dorsal view with prominent bulges on hypotheca and possibly smaller bulges on epitheca. **f** Right lateral view with bulge on hypotheca. **g** Antapical view with prominent bulge on plate 2⁗ and smaller bulge on plate 5‴. **h** Apical view of a cell with bulge on plate 4′. **j** Lateral view of a cell with bulges on epi- and hypotheca. Plate labelling follows the Kofoidean notation, n′: apical plate; n″: precingular plate; n‴: postcingular plate; n⁗: antapical plate; na: anterior intercalary plate. Scale bar = 10 µm

(mean, 40 µm; median, 39 µm; SD, 5 µm; $n = 50$) and their width from 26 to 44 µm (mean, 34 µm; median, 33 µm; SD, 4 µm; $n = 50$). Some of the coccoid cells, either one or two, were observed in an empty theca (Fig. 3d). The fate of such cells could not be determined.

Phylogenetically related strains

All strains showed flagellated, thecate cells (Fig. 5a–d) and coccoid cells (Fig. 5e–f), with the flagellated cells being predominant. The strains were indistinguishable in gross

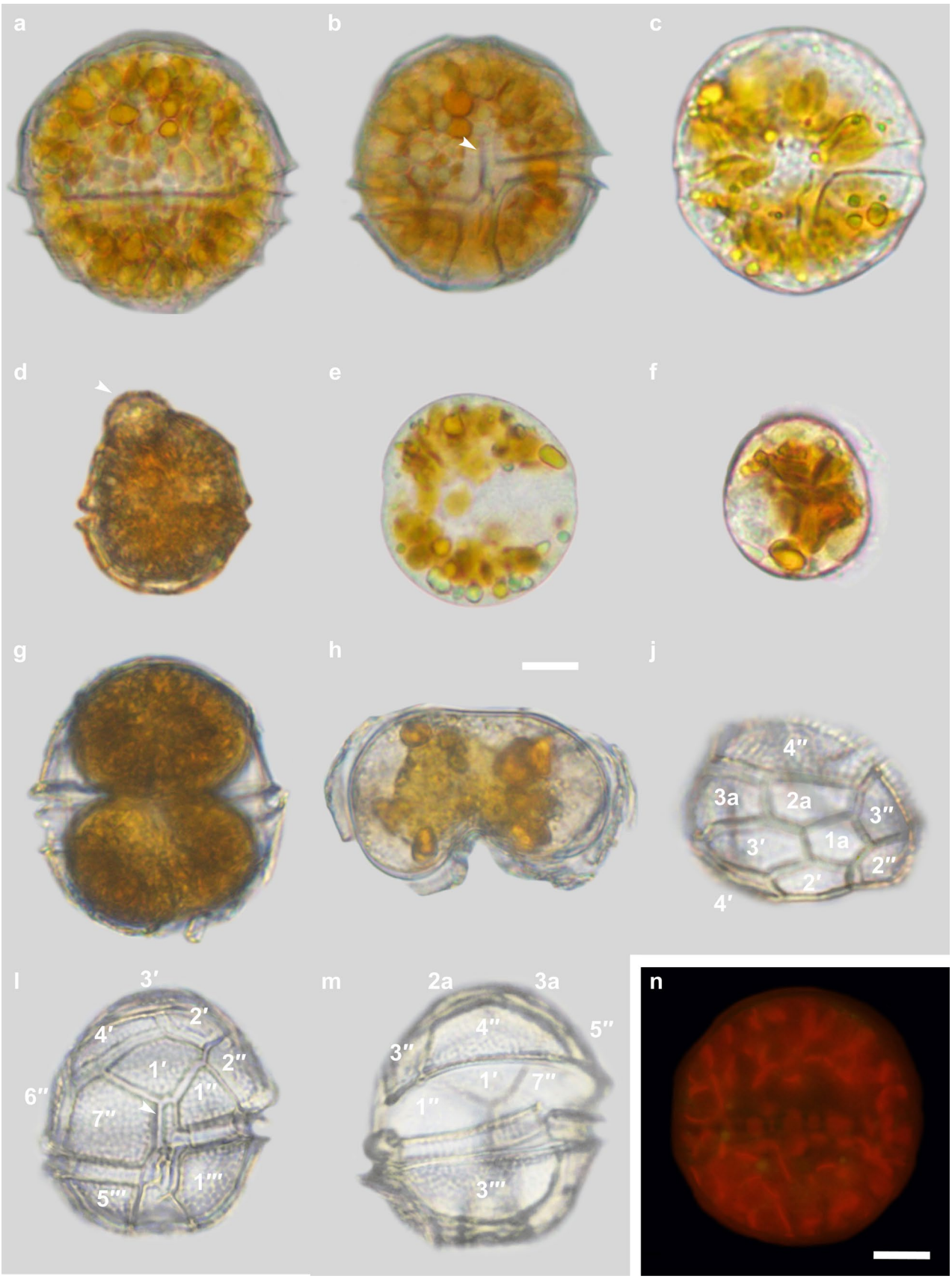
a
b
c
d
e
f
g
h
j
4″
3a
2a
3″
3′
1a
2″
2′
4′
l
3′
2′
4′
1′
2″
6″
1″
7″
1‴
5‴
m
2a
3a
4″
5″
3″
1′
7″
1″
3‴
n

◂**Fig. 5** Cells of phylogenetically related strains (light microscopy). **a** Thecate cell in dorsal view. **b** Thecate cell in ventral view, note the sulcus extending onto the epitheca (arrow). **c** Putatively necrotic, thecate cell. **d** Thecate cell with one bulge on the epitheca (arrow), note that this was the only such cell among thousands of inspected cells. **e**, **f** Coccoid cells, apparently without thecae. **g** Two thecate cells enclosed in the parental theca. **h** Two connected, immotile cells enclosed in the parental thecae. **j** Lid of epitheca in dorsal-apical view (mirrored), composed of plates 2′–4′, all intercalary plates and plates 2″–6″. **l**–**m** Same opened theca in ventral view (**l**) and dorsal view (**m**), note the sulcus extending onto the epitheca (arrow), the dorsal opening and all apical and all intercalary plates and plates 3″–5″ remaining with the hypotheca. **n** Chloroplasts (as inferred from autofluorescence), note the space occupied by the nucleus. Plate labelling follows the Kofoidean notation, n′: apical plate; n″: precingular plate; n‴: postcingular plate; na: anterior intercalary plate. Scale = 10 µm

morphology and are described here cumulatively. Thecate cells were mostly motile (Fig. 5a–d), but they could also be immotile (Fig. 5g–h) lying on the ground of the culture vessels. This phenomenon became more abundant towards the stationary growth phase. The cells were circular in outline and dorsoventrally compressed (Fig. 5a–c). They possessed a large number of golden-brown chloroplasts (colour in varying intensity: Fig. 5a–h) evenly distributed over the cell but leaving space for the nucleus (Fig. 5n). Only necrotic cells showed a grey through dark colouration of the plastids (similar to Fig. 4d). The nucleus was semi-anular (rectangular with rounded angles in outline of dorso-ventral view) and had a median, horizontal position (similar to Fig. 2d).

An apical pore was absent in all thecate cells, and the surface of the cellulosic thecal plates was areolate (Fig. 5j–m). The sulcus extended onto the epitheca as a narrow slit (Fig. 5b, l). The epithecal plate pattern was asymmetrical and presented the Kofoidean formula 4′, 3a, 7″ (Fig. 5j). The size of thecate cells (all strains) ranged from 24 to 61 µm in length (mean = 44 µm, SD = 4.8 µm, n = 350) and from 22 to 58 µm in width (mean = 41 µm, SD = 5.3 µm, n = 350; separate measurement for individual strains are provided as Fig. S1). Among ca. 2800 inspected cells, there was a single individual with a structure similar to a bulge on the epitheca (Fig. 5d).

Rarely, two connected cells, each in its own thecate shell, were observed (Fig. 5h). Cell division was by eleuteroschisis, always with two daughter cells enclosed in a parental theca (Fig. 5g), and began on the dorsal side of the cell (Fig. 5l–m). During thecal opening, epithecal plates disintegrated frequently into separated pieces and only in some cases, larger parts remained intact. The predominant lid was comprised of plates 2′–4′, all intercalary plates and plates 2″–6″ (n = 26, Fig. 5j) and as the other piece the hypotheca, the cingular plates and plates 1′, 1″ and 7″.

Coccoid cells were rare (3%, n = 2800), almost circular in outline and had a smooth surface (Fig. 5e, f). In general, they were smaller than the thecate cells, ranging from 21 to 68 µm (mean, 36 µm; median, 34 µm; SD, 10 µm; n = 50) in length and from 19 to 63 µm (mean, 33 µm; median, 32 µm; SD, 9 µm; n = 50) in width. They were formed intrathecately and were released by ecdysis, but the fate of such cells could not be observed.

Molecular phylogenetics

The SSU + ITS + LSU alignment was 1802 + 684 + 2511 bp long and composed of 329 + 342 + 466 parsimony-informative sites (23%, mean of 16.97 per terminal taxon) and 1920 distinct RAxML alignment patterns. Conflicting topologies in separate analyses of the different rRNA regions were not observed. Figure 6 shows the best-scoring ML tree (− ln = 21,884.93), with the majority of nodes showing high if not maximal support. The Peridiniaceae were monophyletic (100LBS, 1.00BPP) and segregated into *Peridinium volzii* Lemmerm. (100LBS, 1.00BPP), *Peridinium willei* Huitf.-Kaas (100LBS, 1.00BPP), *Peridinium bipes* F.Stein (83LBS, 0.98BPP), *Peridinium limbatum* (A.Stokes) Lemmerm. (100LBS, 1.00BPP), *P. gatunense* (single accession) and *P. cinctum* (98LBS, 1.00BPP).

Peridinium cinctum segregated into seven (two of which new) ITS ribotypes, namely rb1 (74LBS, 0.96BPP), rb2 (69LBS), rb3 (100LBS, 1.00BPP), rb4 (100LBS), rb5 (100LBS, 1.00BPP), rb6 (single accession) and rb7 (100LBS, 1.00BPP). The distinction between rb1 and rb2 was not very clear in the molecular tree but additionally to two differing positions, rb2 showed a 13 bp long deletion in the beginning of the ITS2 loop region by comparison to all other ribotypes including rb1. In the V4 region of the SSU, rb6 differed from rb1, rb2, rb3 and rb4 in 2 positions and rb1 and rb2 from rb3, rb4 and rb6 in 3 positions (data for other ribotypes not available). Sequence variability among ribotypes was also present in the LSU D1/D2 region, totalling 15 positions in the alignment. No compensatory base substitutions or altered secondary structures were identified among the ITS ribotypes assigned to *P. cinctum*. No correlation between phylogeny of *P. cinctum* and biogeography could be stated but occasionally, different ribotypes were detected from the same locality (e.g., GeoM*978: rb2, GeoM*981: rb1, GeoM*979: rb6 from Lake Wojnowickie in June 2018).

Discussion

Strain GeoM*979 shows a morphology similar to *Peridinium tuberosum*

Thousands of cells from multiple strains have been observed in cultured material of *P. cinctum* (Izquierdo López et al., 2018; Romeikat et al., 2019), but never with any kind of protuberance on the hypotheca. With its cells having

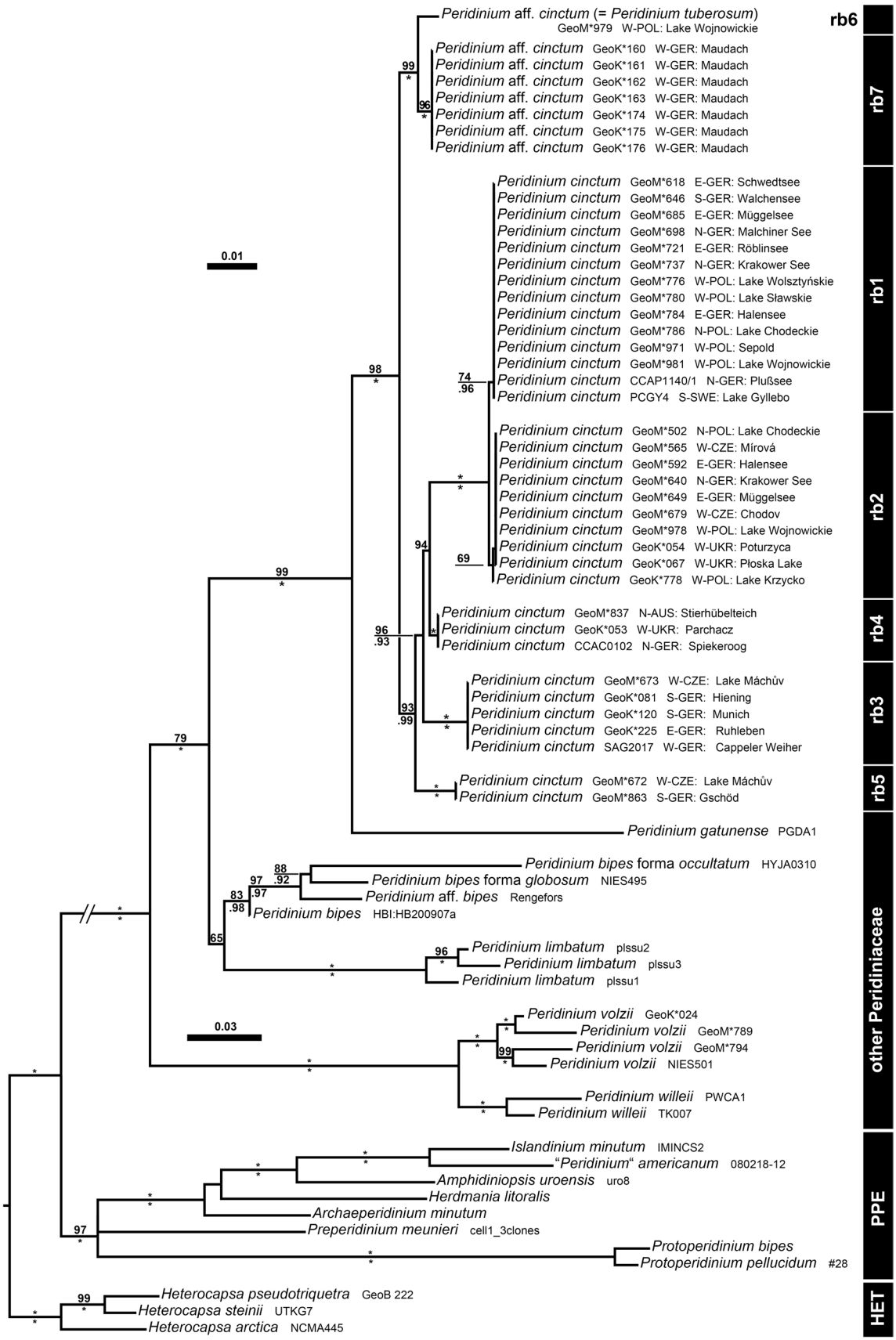
Peridinium aff. cinctum (= Peridinium tuberosum) GeoM*979 W-POL: Lake Wojnowickie
Peridinium aff. cinctum GeoK*160 W-GER: Maudach
Peridinium aff. cinctum GeoK*161 W-GER: Maudach
Peridinium aff. cinctum GeoK*162 W-GER: Maudach
Peridinium aff. cinctum GeoK*163 W-GER: Maudach
Peridinium aff. cinctum GeoK*174 W-GER: Maudach
Peridinium aff. cinctum GeoK*175 W-GER: Maudach
Peridinium aff. cinctum GeoK*176 W-GER: Maudach
Peridinium cinctum GeoM*618 E-GER: Schwedtsee
Peridinium cinctum GeoM*646 S-GER: Walchensee
Peridinium cinctum GeoM*685 E-GER: Müggelsee
Peridinium cinctum GeoM*698 N-GER: Malchiner See
Peridinium cinctum GeoM*721 E-GER: Röblinsee
Peridinium cinctum GeoM*737 N-GER: Krakower See
Peridinium cinctum GeoM*776 W-POL: Lake Wolsztyńskie
Peridinium cinctum GeoM*780 W-POL: Lake Sławskie
Peridinium cinctum GeoM*784 E-GER: Halensee
Peridinium cinctum GeoM*786 N-POL: Lake Chodeckie
Peridinium cinctum GeoM*971 W-POL: Sepold
Peridinium cinctum GeoM*981 W-POL: Lake Wojnowickie
Peridinium cinctum CCAP1140/1 N-GER: Plußsee
Peridinium cinctum PCGY4 S-SWE: Lake Gyllebo
Peridinium cinctum GeoM*502 N-POL: Lake Chodeckie
Peridinium cinctum GeoM*565 W-CZE: Mírová
Peridinium cinctum GeoM*592 E-GER: Halensee
Peridinium cinctum GeoM*640 N-GER: Krakower See
Peridinium cinctum GeoM*649 E-GER: Müggelsee
Peridinium cinctum GeoM*679 W-CZE: Chodov
Peridinium cinctum GeoM*978 W-POL: Lake Wojnowickie
Peridinium cinctum GeoK*054 W-UKR: Poturzyca
Peridinium cinctum GeoK*067 W-UKR: Płoska Lake
Peridinium cinctum GeoK*778 W-POL: Lake Krzycko
Peridinium cinctum GeoM*837 N-AUS: Stierhübelteich
Peridinium cinctum GeoK*053 W-UKR: Parchacz
Peridinium cinctum CCAC0102 N-GER: Spiekeroog
Peridinium cinctum GeoM*673 W-CZE: Lake Máchův
Peridinium cinctum GeoK*081 S-GER: Hiening
Peridinium cinctum GeoK*120 S-GER: Munich
Peridinium cinctum GeoK*225 E-GER: Ruhleben
Peridinium cinctum SAG2017 W-GER: Cappeler Weiher
Peridinium cinctum GeoM*672 W-CZE: Lake Máchův
Peridinium cinctum GeoM*863 S-GER: Gschöd
Peridinium gatunense PGDA1
Peridinium bipes forma occultatum HYJA0310
Peridinium bipes forma globosum NIES495
Peridinium aff. bipes Rengefors
Peridinium bipes HBI:HB200907a
Peridinium limbatum plssu2
Peridinium limbatum plssu3
Peridinium limbatum plssu1
Peridinium volzii GeoK*024
Peridinium volzii GeoM*789
Peridinium volzii GeoM*794
Peridinium volzii NIES501
Peridinium willeii PWCA1
Peridinium willeii TK007
Islandinium minutum IMINCS2
"Peridinium" americanum 080218-12
Amphidiniopsis uroensis uro8
Herdmania litoralis
Archaeperidinium minutum
Preperidinium meunieri cell1_3clones
Protoperidinium bipes
Protoperidinium pellucidum #28
Heterocapsa pseudotriquetra GeoB 222
Heterocapsa steinii UTKG7
Heterocapsa arctica NCMA445
0.01
0.03
rb6
rb7
rb1
rb2
rb4
rb3
rb5
other Peridiniaceae
PPE
HET

◂**Fig. 6** A molecular phylogeny of 56 systematically representative Peridiniaceae, including 42 accessions assignable to *P. cinctum* from various geographic regions. Maximum likelihood tree (– ln = 21,884.93), as inferred from a rRNA nucleotide alignment (1137 parsimony-informative sites) and with strain number information. Numbers on branches are ML bootstrap (above) and Bayesian support values (below) for the clusters (asterisks indicate maximal support values, values under 50 and 0.90, respectively, are not shown). Clades are indicated (*CZE* Czech Republic, *E* East, *GER* Germany, *HET* Heterocapsaceae, *N* North, *PPE* Protoperidiniaceae, *POL* Poland, *rbn* ribotype n, *S* South, *SWE* Sweden, *UKR* Ukraine, *W* West)

bulges of various positions and shapes on the surface, strain GeoM*979 is thus unique but otherwise presents a morphology that is consistent with *P. cinctum*. The chance that the previous studies have overlooked cells with such a distinct trait is nearly impossible, and it is notably also absent from material likewise collected at Lake Wojnowickie at the same time (i.e., GeoM*978, GeoM*981). So far, five different ribotypes have been detected in association with *P. cinctum* (all without bulges: Izquierdo López et al., 2018) and notably, any protuberance is absent even from cells exhibiting a new ribotype, which is presented in this study and shows a close relationship to strain GeoM*979. Albeit rare, the bulges on the hypotheca are a consistent trait of strain GeoM*979 based on the inspection of thousands of cells in all stages of growth. They are neither an artefact (i.e., corresponding cells are viable just like the remaining regular cells) nor an abnormality formed due to environmental conditions (i.e., being the same as for the strains having cells without bulges). Therefore, the occasional phenotype of strain GeoM*979 is likely fixed in its genotype.

Of the *P. cinctum* species group with an asymmetrical epitheca (Moestrup & Calado, 2018), two taxa are conceivable to represent our observation of strain GeoM*979 having bulges of various positions and shapes, namely *P. tuberosum* (Meunier, 1919) and *Peridinium gatunense* var. *carinatum* (Steinecke & Er.Lindem.) Moestrup & Calado (Steinecke & Lindemann, 1923). The latter has an asymmetrical epitheca (like *P. cinctum*) and comb-like flanges (Steinecke & Lindemann, 1923) on the posterior end of the cell (Fig. 7). In fact, the illustrations provided by Meunier (1919) and Steinecke and Lindemann (1923) appear similar (Lindemann, 1928) at first glance, and it is the sulcus that helps to distinguish both taxa (Moestrup & Calado, 2018): In cells of *P. gatunense* and its varieties, it does not extend onto the epitheca, but it does so in *P. cinctum*. Each cell observed of strain GeoM*979 has its sulcus extending onto the epitheca and hence, we can exclude the possible identification of this strain with *P. gatunense* var. *carinatum*. However, plate 1′ is smaller in *P. gatunense* than in *P. cinctum*, and *P. gatunense* var. *carinatum* would have a considerably large such plate for this species.

Beyond *P. gatunense* var. *carinatum*, the question remains, whether cells of strain GeoM*979 correspond to those described by Meunier (1919). Both the original illustrations (Fig. 1) and the cells of strain GeoM*979 have bulges positioned at the posterior end, and their epitheca tabulation pattern is identical. However, strain GeoM*979 exhibits traits that Meunier (1919) did not observe: Cells with bulges show variability in the number and their positions. Meunier (1919), and subsequently also Graffius (1966), consistently presented and drew three bulges on the hypotheca, whereas cells of strain GeoM*979 have—if present—predominantly two bulges. Moreover, cells of strain GeoM*979 occasionally display bulges on the epitheca only or on both hemispheres. In the original illustrations (Fig. 1), the bulges appear generally smaller arising from the centre of a thecal plate, whereas in the living material, the bigger bulges more or less occupy the entire plate.

It should be noted that Meunier (1919) observed field material and was, therefore, silent about possible

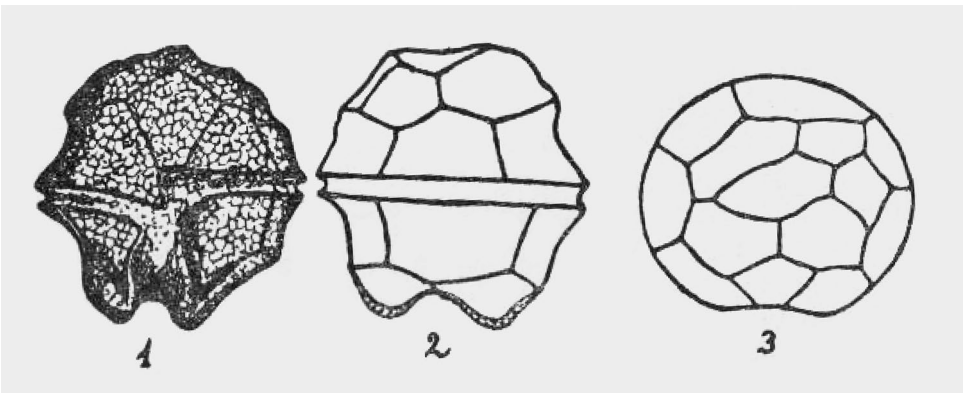

Fig. 7 Original material of *Peridinium gatunense* var. *carinatum* (Steinecke & Lindemann, 1923), note the bulges on the hypotheca and that the sulcus does not extend onto the epitheca. (1) Ventral view with two bulges on hypotheca. (2) Dorsal view with two bulges on hypotheca having comb-like flanges. (3) Apical view with asymmetrical plate pattern, as it is characteristic for the *Peridinium cinctum* species group (Moestrup & Calado, 2018)

intraspecific variability. Particularly, it remains unclear whether single unusual cells of a population otherwise appearing as *P. cinctum* were observed; and whether the illustrations correspond to one cell depicted from several views, or to different cells always showing the same position and number of bulges on the cells' surface; and how abundant the morphology was—overall, it remains the question of a rarely documented species consistently and not only sporadically showing three bulges on the posterior end of the cell. Anyhow, the differences between the historical and our living material cause reluctance to identify cells of strain GeoM*979 as *P. tuberosum*. To clarify its taxonomy, new biological material should be collected at the type locality in Belgium.

Developments

Eleutheroschisis is the regular division type of peridinialean dinophytes (Fensome et al., 1993; Moestrup & Calado, 2018). In *Peridinium*, regular mitosis may take place by usually two cells formed within a parental theca (Schilling, 1891; Lindemann, 1929; Lefèvre, 1932; Dürr, 1979a; *de facto* a sporocyst), and this is confirmed here for all strains under investigation. However, the thecal opening shows variation: The lid of strain GeoM*979 appears identical to the observations of Boltovskoy (1975) and Dürr (1979a) for *P. cinctum* and of Holzer et al. (2022) for *P. volzii*, but the lids of the other strains under study include additionally at least plates 2′ and 4′. Notably, this conformation corresponds to previous observations of more cultured material of *P. cinctum*, irrespectively of the ribotype (Izquierdo López et al., 2018; Romeikat et al., 2019).

Life history or metagenesis of Peridiniaceae is complex and not fully understood at present, but *P. cinctum* is considered isogamous and homothallic (Dürr, 1979b; Pfiester, 1975; Spector et al., 1981). Sexual processes can be induced in cultivation by using nitrogen-deficient media, but zygotes (at least in *P. willei*: Pfiester, 1976) can also be observed in the field (i.e., with regular nitrogen supply). Parental thecae with two viable daughter cells inside could represent also (mitotic) gamete formation (*de facto* a gametocyst, morphologically indistinguishable from the sporocyst described above) if such cells would fuse after release.

The two observed cells, swimming together and having two longitudinal flagella, are most likely fusing gametes (previously illustrated also in SEM: Dürr, 1979a), and at least some of the cells presented here can be associated with sexual processes of *P. cinctum*. In a multi-step process, they develop over a planozygote to a hypnozygote by size increase, loss of mobility and perpetuation of the thecal plate covering and to overcome uncomfortable ecological conditions (Boltovskoy, 1975; Dürr, 1979b; Pfiester, 1975; Spector et al., 1981). Notably, the warty appearance of late hypnozygotes (Pfiester, 1975; Pfiester & Skvarla, 1980) resembles to some degree the cells described by Meunier (1919). Exact cell size is not provided with the protologue (though being in the same range as *P. willei* likewise depicted on the plate), but hypnozygotes are in any case much bigger than the cells with bulges presented here.

The formation of coccoid cells such as the hypnozygotes ('cysts': Stosch, 1973; Dale, 1983) has been improvidently interpreted as (diploid) part of (obligate) life history. However, morphologically different coccoid cells (again intrathecately, but solitary formed) have been additionally reported for *P. cinctum* (Dangeard, 1939; Eren, 1969; Pfiester, 1975). They are smaller than the hypnozygotes, have no indication of thecal plates and are confirmed here as well [but never in combination with the development of extensive mucilage as reported from *Peridinium cinctum* forma *westii* (Lemmerm.) Er.Lindem.: Virieux, 1914]. Such coccoid cells may represent the haploid stage (e.g., as a facultative dormant stage) like the regular thecate cells, as has been suggested for *P. volzii* (Holzer et al., 2022). A single flagellated cell germinates from such coccoid cell (Eren, 1969) by an archaeopyle and a process unknown so far.

Taxonomic delimitation in Peridiniaceae

Species of the Peridiniaceae appear different from other dinophytes regarding the taxonomic delimitation based on DNA sequence data. In fact, 97% of dinophyte species can be identified based on combined ITS + LSU sequence data (Ott et al., 2022), but species of *Peridinium* show a considerable variation of rRNA sequences even within species (Gottschling et al., 2020; Holzer et al., 2022; Izquierdo López et al., 2018). The branches within *P. cinctum* (i.e., including also sequences of strain GeoM*979) are of comparable length like in the other species of *Peridinium* with more than one accession included (i.e., *P. bipes*, *P. limbatum*, *P. volzii*, *P. willei*) that the status of a taxonomically distinct *P. tuberosum* is at least challenged. *Peridinium* appears similar in this respect to other dinophytes such as *Alexandrium* Balech (Kremp et al., 2014) and *Ostreopsis* E.J.Schmidt (Nguyen-Ngoc et al., 2021) from the Gonyaulacales.

In the phylogenetic DNA tree, strain GeoM*979 together with other strains constitute the sister lineage of a core cluster up to now associated with *P. cinctum*. The unusual morphology presented here is found in this lineage only, and this could be indicative of its taxonomic status as a separate species. However, the trait of bulges on the posterior cell's surface is truly rare, and the majority of cells (also of the related strains) shows a morphology indistinguishable from *P. cinctum* (Izquierdo López et al., 2018; Romeikat et al., 2019). Similarly, the epithecal opening does not have the potential to delimitate *P. cinctum*, the lineage including GeoM*979 and other species of *Peridinium* (which should be studied in more detail regarding

this trait anyway). The lack of compensatory base substitutions in the ITS sequences of the strains studied here may also argue for a single, morphologically and molecularly variable species (Coleman, 2009). A separate species, if accepted, could be reliably identified by DNA sequence information only and from a practical perspective, the remaining supposedly cryptic species (Gottschling et al., 2005; Litaker et al., 2009; Montresor et al., 2003; Wang et al., 2019) with a morphology consistent with *P. cinctum* are difficult or even not to recognise at all in the field. We decided to determine the strain GeoM*979 (and the phylogenetically related strains) as *Peridinium* aff. *cinctum*, as long as the true taxonomic status remains elusive. It cannot be excluded that in fact, *P. tuberosum* is a heterotypic synonym of *P. cinctum* (Moestrup & Calado, 2018).

Supplementary Information The online version contains supplementary material available at https://doi.org/10.1007/s13127-023-00635-6.

Acknowledgements Paweł M. Owsianny (Piła), Corinna Romeikat, Sophia Schottenhammel (both Munich) and Beatrix Zierach (Berlin) supported us in the field and/or established new strains, which is gratefully acknowledged here. We thank Eva Facher and Moritz Pretzsch (both Munich) for assistance in the lab, Marina Stark (Munich) for providing an image of a permanent slide, Anna Müller (Munich) for valuable advice of image processing and Rafael Matysiuk (Munich) for providing the computational power for the phylogenetic analyses. The lessons of John McNeill (Edinburgh) and Nicholas Turland (Berlin) on the correct application of the ICN are gratefully acknowledged here.

Funding Open Access funding enabled and organized by Projekt DEAL. This work was supported by the Deutsche Forschungsgemeinschaft (grant GO1459 10–1).

Data availability The datasets generated during and/or analysed during the current study are available in the GenBank repository, https://www.ncbi.nlm.nih.gov/genbank/ (full vouchers are provided in the Supplementary Information).

Declarations

Competing interests The authors declare no competing interests.

References

Annenkova, N. V., Hansen, G., Moestrup, Ø., & Rengefors, K. (2015). Recent radiation in a marine and freshwater dinoflagellate species flock. *ISME Journal, 9*, 1821–1834.

Baykal, T., & Açıkgöz, İ. (2004). Hirfanlı Baraj Gölü Algleri. *Ahi Evran Üniversitesi Kırşehir Eğitim Fakültesi Dergisi, 5*, 115–136.

Baykal, T., Açıkgöz, İ, Yıldız, K., & Bekleyen, A. (2004). A study on algae in Devegeçidi Dam Lake. *Turkish Journal of Botany, 28*, 457–472.

Boltovskoy, A. (1975). Estructura y estereoultrastructura tecal de dinoflagelados. II. *Peridinium cinctum* (Müller) Ehrenberg. *Physis Sección B, 34*, 73–84.

Burkholder, J. M., & Glibert, P. M. (2006). Intraspecific variability: An important consideration in forming generalisations about toxigenic algal species. *African Journal of Marine Science, 28*, 177–180.

Carty, S. (2008). *Parvodinium* gen. nov. for the umbonatum group of *Peridinium* (Dinophyceae). *Ohio Journal of Science, 108*, 103–107.

Coleman, A. W. (2009). Is there a molecular key to the level of "biological species" in eukaryotes? A DNA guide. *Molecular Phylogenetics and Evolution, 50*, 197–203.

Dale, B. (1983). Dinoflagellate resting cysts: "Benthic plankton." In G. A. Fryxell (Ed.), *Survival strategies of the algae* (pp. 69–136). Cambridge University Press.

Dangeard, P. A. (1939). Second mémoire sur la famille des Péridiniens. *Le Botaniste, 29*, 267–308.

Dürr, G. (1979a). Elektronenmikroskopische Untersuchungen am Panzer von Dinoflagellaten. II: *Peridinium cinctum*. *Archiv für Protistenkunde, 122*, 88–120.

Dürr, G. (1979b). Elektronenmikroskopische Untersuchungen am Panzer von Dinoflagellaten. III: Die Zyste von *Peridinium cinctum*. *Archiv für Protistenkunde, 122*, 121–139.

Ehrenberg, C. H. G. (1832). Beiträge zur Kenntnis der Organisation der Infusorien und ihrer geographischen Verbreitung. *Abhandlungen der Königlichen Akademie der Wissenschaften in Berlin, 1830*, 1–88.

Eren, J. (1969). Studies on development cycle of *Peridinium cinctum* f. *westii*. *Internationale Vereinigung für Theoretische und Angewandte Limnologie: Verhandlungen, 17*, 1013–1016.

Fensome, R. A., Taylor, F. J. R., Norris, G., Sarjeant, W. A. S., Wharton, D. I., & Williams, G. L. (1993). *A classification of living and fossil dinoflagellates (Micropaleontology, Special Publication Number 7)*. Sheridan Press.

Gottschling, M., Chacón, J., Žerdoner Čalasan, A., Neuhaus, St., Kretschmann, J., Stibor, H., & John, U. (2020). Phylogenetic placement of environmental sequences using taxonomically reliable databases helps to rigorously assess dinophyte biodiversity in Bavarian lakes (Germany). *Freshwater Biology, 65*, 193–208.

Gottschling, M., Keupp, H., Plötner, J., Knop, R., Willems, H., & Kirsch, M. (2005). Phylogeny of calcareous dinoflagellates as inferred from ITS and ribosomal sequence data. *Molecular Phylogenetics and Evolution, 36*, 444–455.

Gottschling, M., & Plötner, J. (2004). Secondary structure models of the nuclear internal transcribed spacer regions and 5.8S rRNA in Calciodinelloideae (Peridiniaceae) and other dinoflagellates. *Nucleic Acids Research, 32*, 307–315.

Gottschling, M., Söhner, S., Zinßmeister, C., John, U., Plötner, J., Schweikert, M., et al. (2012). Delimitation of the Thoracosphaeraceae (Dinophyceae), including the calcareous dinoflagellates, based on large amounts of ribosomal RNA sequence data. *Protist, 163*, 15–24.

Graffius, J. H. (1966). Additions to our knowledge of Michigan Pyrrhophyta and Chloromonadophyta. *Transactions of the American Microscopical Society, 85*, 260–270.

Guillard, R. R., & Lorenzen, C. J. (1972). Yellow-green algae with chlorophyllide c. *Journal of Phycology, 8*, 10–14.

Hebert, P. D. N., Cywinska, A., Ball, S. L., & DeWaard, J. R. (2003). Biological identifications through DNA barcodes. *Proceedings of the Royal Society B-Biological Sciences, 270*, 313–321.

Höll, K. (1928). *Oekologie der Peridineen. Studien über den Einfluß chemischer und physikalischer Faktoren auf die Verbreitung der Dinoflagellaten im Süßwasser*. Fischer.

Holzer, V. J. C., Kretschmann, J., Knechtel, J., Owsianny, P. M., & Gottschling, M. (2022). Morphological and molecular variability of *Peridinium volzii* Lemmerm. (Peridiniaceae, Dinophyceae) and its relevance for infraspecific taxonomy. *Organisms Diversity & Evolution, 22*, 1–15.

Izquierdo López, A., Kretschmann, J., Žerdoner Čalasan, A., & Gottschling, M. (2018). The many faces of *Peridinium cinctum*: Morphological and molecular variability in a common dinophyte. *European Journal of Phycology, 53*, 156–165.

Janofske, D. (1992). Kalkiges Nannoplankton, insbesondere Kalkige Dinoflagellaten-Zysten der alpinen Ober-Trias: Taxonomie, Biostratigraphie und Bedeutung für die Phylogenie der Peridiniales. *Berliner Geowissenschaftliche Abhandlungen (E), 4*, 1–53.

Kremp, A., Tahvanainen, P., Litaker, W., Krock, B., Suikkanen, S., Leaw, C. P., et al. (2014). Phylogenetic relationships, morphological variation, and toxin patterns in the *Alexandrium ostenfeldii* (Dinophyceae) complex: Implications for species boundaries and identities. *Journal of Phycology, 50*, 81–100.

Kretschmann, J., Owsianny, P. M., Žerdoner Čalasan, A., & Gottschling, M. (2018). The hot spot in a cold environment: Puzzling *Parvodinium* (Peridiniopsidaceae, Peridiniales) from the Polish Tatra Mountains. *Protist, 169*, 206–230.

Kretschmann, J., Žerdoner Čalasan, A., Knechtel, J., Owsianny, P. M., Facher, E., & Gottschling, M. (2022). Evolution of Thoracosphaeroideae (Peridiniales, Dinophyceae) and a case of atavism in taxonomically clarified *Chimonodinium lomnickii* var. *wierzejskii* from the Polish Tatra Mountains. *European Journal of Phycology, 57*, 406–421.

Kretschmann, J., Žerdoner Čalasan, A., Kusber, W.-H., & Gottschling, M. (2018). Still curling after all these years: *Glenodinium apiculatum* Ehrenb. (Peridiniales, Dinophyceae) repeatedly found at its type locality in Berlin (Germany). *Systematics and Biodiversity, 16*, 200–209.

Киселев, И. А. (1950). *Панцирные жгутиконосцы (Dinoflagellata) морей и пресных вод СССР*. Москва́: Академии Наук СССР.

Lefèvre, M. M. (1932). Monographie des espèces du genre *Peridinium*. *Archives de Botanique, 2*, 1–210.

Lindemann, E. B. L. W. (1917). Beiträge zur Kenntnis des Seenplanktons der Provinz Posen. (Südwestposener Seengrupe.) II. *Zeitschrift der Naturwissenschaftlichen Abteilung der Deutschen Gesellschaft für Kunst und Wissenschaft in Posen, 24.3*, 2–41.

Lindemann, E. B. L. W. (1920). Untersuchungen über Süßwasserperidineen und ihre Variationsformen II. *Archiv für Naturgeschichte, 84*, 121–194.

Lindemann, E. B. L. W. (1928). Vorläufige Mitteilung. *Archiv für Protistenkunde, 63*, 259–260.

Lindemann, E. B. L. W. (1929). Experimentelle Studien über die Fortpflanzungserscheinungen der Süßwasserperidineen auf Grund von Reinkulturen. *Archiv für Protistenkunde, 68*, 1–104.

Litaker, R. W., Vandersea, M. W., Faust, M. A., Kibler, S. R., Chinain, M., Holmes, M. J., et al. (2009). Taxonomy of *Gambierdiscus* including four new species, *Gambierdiscus caribaeus*, *Gambierdiscus carolinianus*, *Gambierdiscus carpenteri* and *Gambierdiscus ruetzleri* (Gonyaulacales, Dinophyceae). *Phycologia, 48*, 344–390.

Manoylov, K. M. (2014). Taxonomic identification of algae (morphological and molecular): Species concepts, methodologies, and their implications for ecological bioassessment. *Journal of Phycology, 50*, 409–424.

Mayr, E. (1942). *Systematics and the origin of species, from the viewpoint of a zoologist*. Columbia University Press.

Meunier, A. (1919). Microplancton de la mer Flamande. 3. Les péridiniens. *Mémoires du Musée Royal d'Histoire Naturelle de Belgique, 8*, 1–116.

Moestrup, Ø., & Calado, A. J. (2018). *Dinophyceae*. Springer.

Montresor, M., Sgrosso, S., Procaccini, G., & Kooistra, W. H. C. F. (2003). Intraspecific diversity in *Scrippsiella trochoidea* (Dinophyceae): Evidence for cryptic species. *Phycologia, 42*, 56–70.

Morrison, W. R., Lohr, J. L., Duchen, P., Wilches, R., Trujillo, D., Mair, M., et al. (2009). The impact of taxonomic change on conservation: Does it kill, can it save, or is it just irrelevant? *Biological Conservation, 142*, 3201–3206.

Nguyen-Ngoc, L., Doan-Nhu, H., Larsen, J., Phan-Tan, L., Nguyen, X. V., Lundholm, N., et al. (2021). Morphological and genetic analyses of *Ostreopsis* (Dinophyceae, Gonyaulacales, Ostreopsidaceae) species from Vietnamese waters with a re-description of the type species. *O. siamensis*. *Journal of Phycology, 57*, 1059–1083.

Ott, B. M., Litaker, R. W., Holland, W. C., & Delwiche, C. F. (2022). Using rDNA sequences to define dinoflagellate species. *PLoS ONE, 17*, e0264143.

Pfiester, L. A. (1975). Sexual reproduction of *Peridinium cinctum* f. *ovoplanum* (Dinophyceae). *Journal of Phycology, 11*, 259–265.

Pfiester, L. A. (1976). Sexual reproduction of *Peridinium willei* (Dinophyceae). *Journal of Phycology, 12*, 234–238.

Pfiester, L. A., & Skvarla, J. J. (1980). Comparative ultrastructure of vegetative and sexual thecae of *Peridinium limbatum* and *Peridinium cinctum* (Dinophyceae). *American Journal of Botany, 67*, 955–958.

Romeikat, C., Izquierdo López, A., Tietze, C., Kretschmann, J., & Gottschling, M. (2019). Typification for reliable application of subspecific names within *Peridinium cinctum* (Peridiniales, Dinophyceae). *Phytotaxa, 424*, 147–157.

Romeikat, C., Knechtel, J., & Gottschling, M. (2020). Clarifying the taxonomy of *Gymnodinium fuscum* var. *rubrum* from Bavaria (Germany) and placing it in a molecular phylogeny of the Gymnodiniaceae (Dinophyceae). *Systematics and Biodiversity, 18*, 102–115.

Schiller, J. (1937). *Rabenhorst's Kryptogamen-Flora. Zweite Auflage. Band 10, Abt. 3, Teil 2. Alt. t.p.: Dinoflagellatae (Peridineae)*. Leipzig: Akademische Verlagsgesellschaft.

Schilling, A. J. (1891). *Die Süsswasser-Peridineen. Flora, 74*, 220–229.

Shams, M., Afsharzadeh, S., & Atici, T. (2012). Seasonal variations in phytoplankton communities in Zayandeh-Rood Dam Lake (Isfahan, Iran). *Turkish Journal of Botany, 36*, 715–726.

Spector, D. L., Pfiester, L. A., & Triemer, R. E. (1981). Ultrastructure of the dinoflagellate *Peridinium cinctum* f. *ovoplanum*. II. Light and electron microscopic observations on fertilization. *American Journal of Botany, 68*, 34–43.

Stein, S. F. N. R. (1883). *Der Organismus der Infusionsthiere nach eigenen Forschungen in systematischer Reihenfolge bearbeitet 3.2*. Leipzig: Engelmann.

Steinecke, F., & Lindemann, E. B. L. W. (1923). Die Mikroflora des Zwergbirkenmoors von Neulinum. *Schriften für Süßwasser- und Meereskunde, 1*, 38–42.

Stern, R. F., Andersen, R. A., Jameson, I., Küpper, F. C., Coffroth, M.-A., Vaulot, D., et al. (2012). Evaluating the ribosomal internal transcribed spacer (ITS) as a candidate dinoflagellate barcode marker. *PLoS ONE, 7*, e42780.

Stosch, H. A. (1973). Observations on vegetative reproduction and sexual life cycles of two freshwater dinoflagellates, *Gymnodinium*

pseudopalustre Schiller and *Woloszynskia apiculata* sp. nov. *British Phycological Journal, 8*, 105–134.

Tillmann, U., Gottschling, M., Nézan, E., Krock, B., & Bilien, G. (2014). Morphological and molecular characterization of three new *Azadinium* species (Amphidomataceae, Dinophyceae) from the Irminger Sea. *Protist, 165*, 417–444.

Tillmann, U., Hoppenrath, M., & Gottschling, M. (2019). Reliable determination of *Prorocentrum micans* Ehrenb. (Prorocentrales, Dinophyceae) based on newly collected material from the type locality. *European Journal of Phycology, 54*, 417–431.

Turland, N. J., Wiersema, J. H., Barrie, F. R., Greuter, W., Hawksworth, D. L., & Herendeen, P. S., et al. (2018). International Code of Nomenclature for algae, fungi, and plants (Shenzhen Code) adopted by the Nineteenth International Botanical Congress Shenzhen, China, July 2017. Glashütten: Koeltz.

Virieux, J. (1914). Sur la reproduction d'un péridinien limnétique, *Peridinium westii* Lemm. *Comptes-Rendus des Séances et Mémoires de la Société de Biologie*. *Paris, 76*, 534–536.

Wang, N., Mertens, K. N., Krock, B., Luo, Z., Derrien, A., Pospelova, V., et al. (2019). Cryptic speciation in *Protoceratium reticulatum* (Dinophyceae): Evidence from morphological, molecular and ecophysiological data. *Harmful Algae, 88*, 101610.

Wilson, E. O. (2017). Biodiversity research requires more boots on the ground. *Nature Ecology & Evolution, 1*, 1590–1591.

Zuker, M. (2003). Mfold web server for nucleic acid folding and hybridization prediction. *Nucleic Acids Research, 31*, 3406–3415.